A Face on Transmembrane Segment 8 of the Lactose Permease Is Important for Transport Activity†

Aileen L. Green and Robert J. Brooker*

Department of Genetics, Cell Biology, and Development and the Bioprocess Technology Institute, University of Minnesota, St. Paul, Minnesota 55108

Received May 2, 2001; Revised Manuscript Received August 8, 2001

ABSTRACT: Previous work on the lactose permease of *Escherichia coli* has shown that mutations along a face of predicted transmembrane segment 2 (TMS-2) play a critical role in conformational changes associated with lactose transport [Green, A. L., Anderson, E. J., and Brooker, R. J. (2000) *J. Biol. Chem. 275*, 23240−23246]. In the current study, mutagenesis was conducted along the side of predicted TMS-8 that contains the first amino acid in the conserved loop 8/9 motif. Several substitutions at positions 261, 265, 272, and 276 were markedly defective for downhill lactose transport although these mutants were well expressed. Substitutions along the entire side of TMS-8 containing the first amino acid in the loop 8/9 motif displayed defects in uphill lactose transport. Again, substitutions at positions 261, 265, 268, 272, and 276 were the most defective, with several of these mutants showing no lactose accumulation against a gradient. According to helical wheel plots, Phe-261, Thr-265, Gly-268, Asn-272, and Met-276 form a continuous stripe along one face of TMS-8. These results are discussed according to our hypothetical model, in which the two halves of the protein form a rotationally symmetrical dimer. In support of this model, alignment of predicted TMS-2 and TMS-8 shows an agreement between the amino acid residues in these transmembrane segments that are critical for lactose transport activities.

The lactose permease is a cytoplasmic integral membrane protein that couples the transport of H^+ and lactose with a 1:1 stoichiometry (*1*, *2*). This symporter is able to couple the inwardly directed H^+ electrochemical gradient to the transport of lactose so that secondary active transport can be achieved with regard to the sugar (*3*, *4*). From the cloning and nucleotide sequence of the *lacY* gene, the lactose permease contains 417 amino acids and has a predicted molecular mass of 46 504 Da (*5*, *6*). Several topological studies are consistent with a secondary structural model in which the lactose permease contains 12 transmembrane segments in an α-helical conformation (*7*−*10*).

The lactose permease is a member of the major facilitator superfamily (MFS) (*11*−*13*). The superfamily members transport a variety of solutes including sugars, amino acids, Krebs cycle intermediates, and antibiotics. Most members of the MFS are predicted to contain 12 membrane-spanning segments by hydrophobicity analysis (*14*). Among members of the superfamily, a general homology exists between the first and second halves of the proteins, consistent with the hypothesis that the superfamily arose by a gene duplication/fusion event of a primordial gene encoding a protein of 6 transmembrane segments (*15*). On the basis of a number of parameters, including hydropathicity, amphipathicity, interhelical loop length, and putative helical interactions in the lactose permease, we proposed a general, three-dimensional arrangement for all 12 transmembrane helices in the superfamily (*14*). Another laboratory has also proposed a model describing the three-dimensional arrangement of the helices based upon cross-linking and biophysical studies (*16*). A distinguishing feature of our hypothetical model is that it shows the two halves of the transporter interacting in a rotationally symmetrical manner to facilitate transport.

A consistent feature of the superfamily is the identification of a conserved motif, GXXX(D/E)(R/K)XG[X](R/K)(R/K), located in hydrophilic loop 2/3 and repeated again at the analogous region in the second half of the protein in loop 8/9 (*11*−*13*) (Figure 1). Although the level of homology within the motif varies among members of the MFS, its conservation within such a large superfamily suggests that it may play a general role in protein structure or function. The importance of the first position in the motif has been extensively studied in the lactose permease and tetracycline antiporter. In the lactose permease, bulky substitutions in the loop 2/3 motif at the first position glycine were found to inhibit the velocity of lactose transport without affecting the affinity for lactose (*17*). Loop 8/9 of the lactose permease has a proline at the first position of the motif (Pro-280) (see Figure 1). A study of the loop 8/9 motif showed that several mutations at position 280 result in defective lactose transport (*18*). Studies by Yamaguchi et al. (*19*) on the conserved loop motifs from the tetracycline antiporter support the finding that the first loop 2/3 motif is critical for transport activity. However, these authors found mutations in the loop 8/9 motif to be less detrimental than similar substitutions in the loop 2/3 motif. Overall, the structural studies of the conserved

† This work was supported by Grant GM53259 from the National Institutes of Health.

* To whom correspondence should be addressed at the Bioprocess Technology Institute, 240 Gortner Laboratories, 1479 Gortner Ave., St. Paul, MN 55108. Tel: 612-624-3053. Fax: 612-625-1700. E-mail: robert-b@biosci.umn.edu.

10.1021/bi0109055 CCC: $20.00
Published on Web 09/12/2001

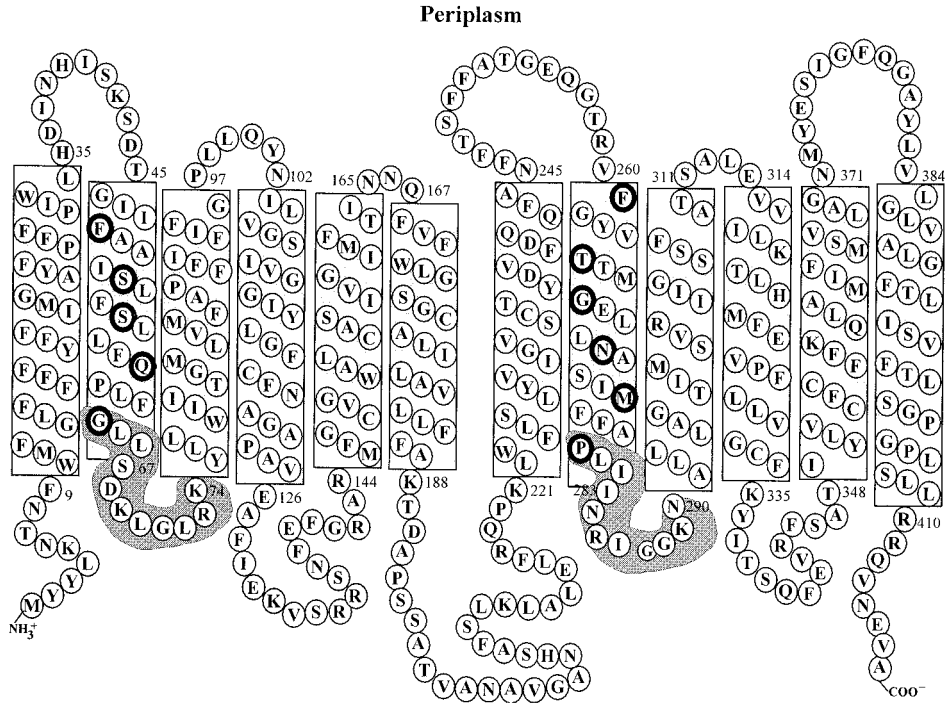

FIGURE 1: Secondary topology of the lactose permease. The boundaries of transmembrane segments were determined by the MEMSAT program (*52*). Four transmembrane segments (5, 6, 7, and 10), which were predicted to be less than 20 amino acids by this program, were extended to a minimum length of 20 amino acids on the basis of alignment with other MFS members. The loop 2/3 and loop 8/9 motifs are highlighted in gray. Amino acids in TMS-2 and TMS-8 that are important for transport velocity are highlighted in black (*18*, *20*, *48*, and this study; see Results).

loop motifs indicate that they may play a role in global conformational changes.

Recently, we identified a face on predicted TMS-2 of the lactose permease containing Phe-49, Ser-53, Ser-56, and Gln-60 that is important for conformational changes (*20*) (Figure 1). Bulky substitutions at these sites have detrimental effects on transport velocity, protein expression, and/or the uphill accumulation of sugar. This critical face of TMS-2 contains the first amino acid of the loop 2/3 motif (Gly-64). In this same study, we also proposed a revised tertiary model of the 12 transmembrane segments of the lactose permease. In our newer model, TMS-2 is shifted more toward the channel opening, whereas predicted transmembrane segment 4 (TMS-4) and transmembrane segment 10 (TMS-10) are shifted slightly away from the channel opening. According to our revised model, the critical face of TMS-2 is located at an interface between the two halves of the protein. Furthermore, the rotational symmetry of our hypothetical model places TMS-8 near the first half of the protein at an interface with transmembrane segment 5 (TMS-5). Given the location of the conserved loop motifs and the critical face of TMS-2 at the interface between the two halves of the protein, we hypothesize that TMS-8 contains a face that is important for conformational changes.

The proximity of TMS-8 to other transmembrane segments has been studied using genetic, biochemical, and biophysical techniques. Hypothetical models place TMS-8 in close proximity to TMS-5 on the basis of cross-linking, site-directed chemical cleavage, and site-directed spin labeling studies (*21*−*23*). Using site-directed excimer fluorescence and site-directed spin labeling of A273C and M299C, Wang et al. (*24*) demonstrated proximity of TMS-8 to transmembrane segment 9 (TMS-9). The residue pairs were chosen because they are one turn of the helix away from residues thought to be ion paired (Glu-269 in TMS-8 and Arg-302 in TMS-9). Proximity has also been shown between TMS-8 and TMS-9 by engineering divalent metal binding sites (bis-His residues) with construction of a R302H/E269H/H322F mutant (*25*). Finally, residue pairs Glu-269 and His-322 have been placed near each other on the basis of site-directed excimer fluorescence and engineered metal binding sites (*26*, *27*). The results of these studies indicate that the face of TMS-8 containing the negatively charged residue (Glu-269) is close to the positively charged residues on TMS-9 and TMS-10.

The face of TMS-8 juxtaposed to TMS-5 includes several residues (Val-264, Gly-268, and Asn-272) sensitive to cysteine replacement that display substrate protection against inactivation and labeling by *N*-ethylmaleimide (*28*) (Figure 2). In contrast, a cysteine in place of Thr-265 on that same face of predicted TMS-8 exhibits a dramatic increase in reactivity with the sulfhydryl label in the presence of substrate, and the increase is blocked by an impermeant thiol reagent. The authors concluded that the face of TMS-8 with Val-264, Gly-268, and Asn-272 is in close proximity to the substrate recognition site, which is believed to contain Cys-148 (TMS-5). Furthermore, it was concluded that Thr-265 is affected by conformational changes elicited by substrate binding. The only TMS-8 mutants displaying less than 10% activity in cysteine scanning mutagenesis were E269C and P280C (*29*).

The role of the charged residue Glu-269 in TMS-8 has been extensively investigated. All nonionizable substitutions at codon 269 are completely defective for active accumulation of sugars (*30*, *31*). The conservative substitution Asp-269 demonstrates the importance of size at this position.

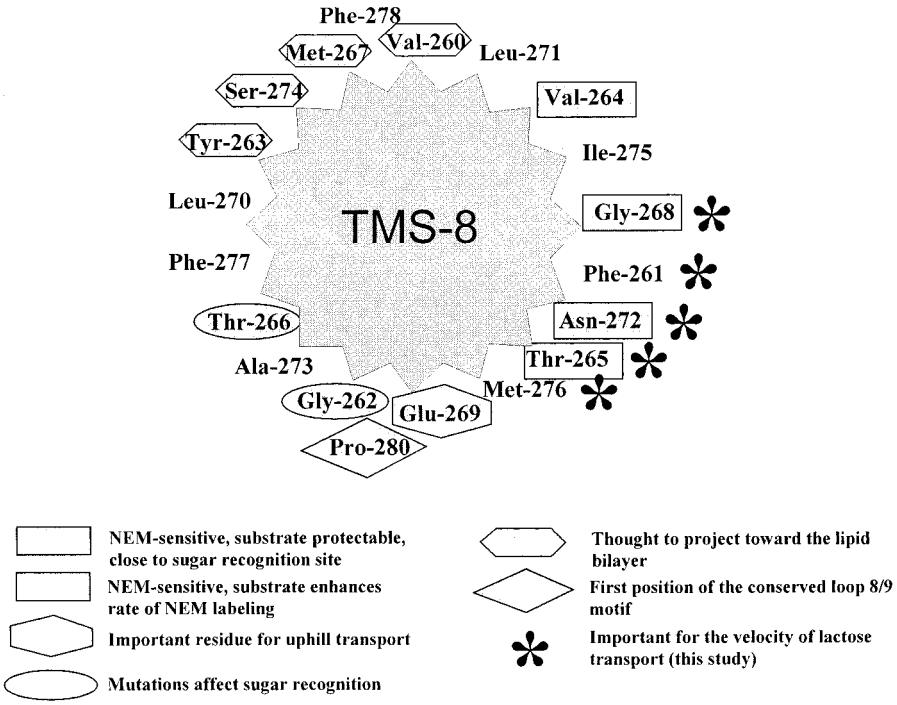

FIGURE 2: Helical wheel plot of transmembrane segment 8. A periplasmic view of a helical wheel plot of TMS-8 from amino acids 261 to 280.

Aspartate differs in size from a glutamate residue by a single methylene group, yet an E269D mutant was unable to accumulate lactose against a concentration gradient (*30*). The size of the negatively charged residue may facilitate its interaction with other charged residues in the lactose permease.

Mutations at Gly-268 have been identified as second-site suppressors of charged mutants displaying slow growth or a white phenotype on MacConkey plates (*32*, *33*). None of the suppressors obtained from these screens (K319N/G268R, E269Q/G268V, and D240A/G268V) were able to accumulate lactose against a concentration gradient. From these suppressor screens, E269Q/T265M was another TMS-8 suppressor identified. Only at high concentrations was a D240A/G268V isolate capable of significant downhill transport. It was thought that these mutants may have poor affinity for the sugar. However, none of the glycine residues in TMS-8 are essential for transport activity as demonstrated by a glycine mutagenesis study by Jung et al. (*34*), which concluded that none of the glycine residues are mandatory for activity.

Finally, mutants have been identified in TMS-8 that show diminished lactose transport or altered sugar recognition (Figure 2). A T266I mutant can transport maltose (*35*), and G262D/C mutants have the ability to grow only on high concentrations of lactose (*35*, *36*). Hinkle et al. (*37*) performed cassette mutagenesis of TMS-8. Using this approach, many multiple mutants were uncovered. However, some single-site mutants (G262V, G268V, E269V, and A273D) were found to be inactive on the basis of their white phenotype on MacConkey plates. A stripe of mutable codons consisting of Val-260, Tyr-263, Met-267, and Ser-274 that retained transport activity was identified in this study, and it was suggested that this "mutable stripe" interacts with the membrane phospholipids (Figure 2). This mutable stripe is located opposite the face of TMS-8 that contains Glu-269.

In this paper we report the results of a mutagenesis study conducted along the side of predicted TMS-8 containing Pro-280. This residue is on the same face that has been shown to interact with TMS-5, although substantial mutagenesis along this face has yet to be carried out. The data are analyzed in terms of a topological model of TMS-8, and we propose a functional role for the conserved loop 8/9 motif. According to our model this face of TMS-8 is located in a rotationally equivalent position to the critical face of TMS-2 identified in our previous study.

MATERIALS AND METHODS

Reagents. Lactose [*O*-β-D-galactopyranosyl-(1,4)-α-D-glucopyranose] and melibiose [*O*-α-D-galactopyranosyl-(1,6)-α−D-glucopyranose] were purchased from Sigma. [^{14}C]-Lactose and Sequenase (version 2.0) were purchased from Amersham Pharmacia Biotech. Restriction enzymes and DNA ligase were purchased from New England BioLabs, Inc. (Beverly, MA). All remaining reagents were of analytical grade.

Bacterial Strains and Methods. The relevant genotypes of the bacterial strains and plasmids are described below in Table 1. Plasmid DNA was purified using the Eppendorf Plasmid Mini DNA Kit (Westbury, NY). Restriction digests and ligations were performed according to the manufacturers' recommendations. Cell cultures were grown in YT media (*38*) supplemented with tetracycline (0.01 mg/mL).

Sugar Transport Assays. Cells were grown at 37 °C with shaking to mid-log phase in YT media supplemented with 5 μg/mL tetracycline and 0.25 mM isopropyl 1-thio-β-D-galactopyranoside. The cells were pelleted by centrifugation at 5000*g* for 5 min, and the resulting pellet was washed in phosphate buffer, pH 7.0, containing 60 mM K_2HPO_4 and 40 mM KH_2PO_4 and then resuspended in the same buffer at a concentration of about 0.5 mg of protein/mL. The cells

Table 1: Bacterial Strains and Plasmids

strain[a]	relevant genotype (chromosome/F′/plasmid)	reference
T184	*lacI*$^+$ *lacO*$^+$ *lacZ*$^-$ *lacY*$^-$/*lacI*^{Q} *lacO*$^+$ *lacZU*^{118} (*lacY*$^-$)/−	*50*
HS4006/F′I^{Q}Z$^+$Y$^-$	Δ(*lac-pro*)Δ*malB101*/*lacI*^{Q} *lacO*$^+$ *lacZ*$^+$ *lacY*$^-$/−	*51*
pAlterLacY[b]	−/−/Δ(*lacI*) *lacO*$^+$Δ(*lacZ*) *lacY*$^+$ Δ(*lacA*) *Tet*^{R}	this study

plasmid[c]	level of protein expression (% WT ± SE)	plasmid[c]	level of protein expression (% WT ± SE)
pAlterLacY (wild-type)	100	pG268V	38 ± 8
		pF261D	152 ± 39
pF278A	94 ± 20	pF261A	110 ± 20
pF278W	39 ± 10	pF261W	191 ± 2
pL271A	160 ± 1	pN272A	143 ± 13
pL271F	29 ± 3	pN272Q	103 ± 17
pL271W	27 ± 9	pN272Y	67 ± 20
pV264A	158 ± 1	pT265A	174 ± 23
pV264C	147 ± 12	pT265S	192 ± 16
pV264F	182 ± 8	pT265Q	175 ± 10
pV264W	14 ± 8	pT265Y	78 ± 21
pI275A	156 ± 9	pM276A	175 ± 18
pI275F	161 ± 3	pM276L	180 ± 17
pI275W	3 ± 3	pM276Y	114 ± 1
pG268A	132 ± 13	pT265Y/M276Y	121 ± 14
pG268S	76 ± 12		
pG268C	101 ± 23		

[a] In strain T184, *lacZU*^{118} is a polar nonsense mutation, which results in a *LacZ*$^-$*LacY*$^-$ phenotype (*50*). [b] pAlterLacY was constructed by cloning the 2300 bp *Eco*RI fragment from pLac184 (*30*), which carries the wild-type *lacY* gene, into the *Eco*RI site of pAlter-1 (Accession Number X65334). The *lacY* gene and the tetracycline resistance gene are in the opposite transcriptional direction. [c] The following plasmids are identical with pAlterLacY except for the noted substitutions within the *lacY* gene.

were equilibrated at 30 °C for 5−10 min before [^{14}C]lactose (1.0 μCi/mL) was added. Aliquots of 100 μL were removed at the appropriate time points, and the cells were captured on 0.45 μm Metricel membranes (Gelman Sciences, Inc., Ann Arbor, MI). The cells were then washed with 5−10 mL of ice-cold phosphate buffer by rapid filtration. The filter with the cells was then placed in liquid scintillation fluid and counted using a Beckman LS1801 liquid scintillation counter. Uphill and downhill transport assays were similar except that a *lacZ* minus strain was used in the uphill assays.

As a negative control, the strain T184/pAlter-1, which lacks a functional *lacY* gene, was also subjected to lactose transport assays. The background values from the T184/pAlter-1 strain were subtracted from the values obtained from the strains carrying the wild-type or mutant *lacY* genes.

For the counterflow experiments, mid-log cells were washed in phosphate buffer (pH 7.0) and resuspended to a density of approximately 0.5 mg of protein/mL. An aliquot of cells was then added to a phosphate buffer solution (pH 7.0) containing 30 mM sodium azide and 20 mM lactose (nonradiolabeled). The cells were incubated at room temperature for 40−60 min to allow the lactose to equilibrate across the membrane. The cells were then centrifuged for 10 min at 6000 rpm in a clinical centrifuge. The supernatant was discarded, and the tube was carefully wiped to remove any remaining liquid. The cell pellet was then resuspended in 900 μL of a 23 °C (Figure 3a) or 16 °C (Figure 3b) assay solution containing 30 mM sodium azide and 0.5 mM [^{14}C]-lactose (0.965 μCi/mL) in 100 mM phosphate buffer at pH 7.0. At the designated time intervals, aliquots were withdrawn and filtered over a membrane filter (pore size = 0.45 μm). The external medium was washed away with 5−10 mL of phosphate buffer (pH 7.0) by rapid filtration. The amount of [^{14}C]lactose retained within the cells was determined by liquid scintillation counting of the membrane filters.

Calculations. The apparent K_m and apparent V_{max} values were determined using the SigmaPlot hyperbolic curve-fitting program by the Jandel Corp. (San Rafael, CA). Briefly, the program calculates a nonlinear least-squares fit of the data on the basis of the Michaelis−Menten equation. The program requires an estimate of the apparent K_m and apparent V_{max} values, which were determined by a Hanes−Woolf plot (*39*). Since the amount of experimental variation was greater for the Western analysis (described below), the apparent V_{max} values were not corrected for variations in expression levels.

Membrane Isolation and Western Blot Analysis. Ten milliliters of mid-log cells grown as for transport assays were harvested by centrifugation (5000*g*, 10 min). The pellet was quickly frozen in liquid nitrogen and resuspended in 800 μL of MTPBS (150 mM NaCl, 16 mM Na_2HPO_4, 4 mM NaH_2PO_4) plus phenylmethanesulfonyl fluoride (0.1 mg/mL) and pepstatin A (1 μg/mL). The suspension was quickly frozen two more times in liquid nitrogen. The cell suspension was then sonicated three times for 20 s each. Triton X-100 was added to a final concentration of 1%, and the membrane fraction was harvested by centrifugation. The pellet was resuspended in 100 μL of MTPBS and subjected to a modified Lowry protein assay (Sigma). A sample of 100 μg of protein was subjected to SDS−polyacrylamide gel electrophoresis using a 12% acrylamide gel. The proteins were electroblotted to nitrocellulose, and Western blot analysis was performed according to Sambrook et al. (*40*). The primary polyclonal antibody recognizes the lactose permease C-terminal 10 amino acids. The secondary antibody, goat anti-rabbit, conjugated to alkaline phosphatase, was purchased from Sigma. The Western blot was then scanned using a Molecular Dynamics laser densitometer and analyzed by comparison to wild-type values for the same preparation and Western blot. As shown below in Table 1, the values are reported as a percentage of wild type for three separate preparations.

Site-Directed Mutagenesis. The plasmid pAlterLacY was created by cloning the 2.3 *Eco*RI fragment from pLac184 (*30*), containing the entire *lacY* gene, into the vector pAlter-1 (Promega, Accession Number X65334). A pAlterLacY plasmid with the *lacY* gene cloned in the opposite transcriptional direction as the tetracyline resistance gene was selected for use. Site-directed mutagenesis was performed using mutagenic polymerase chain reaction primers, which spanned a *Bcl*I site located at codons 281−283 within the *lacY* gene. A mutagenic primer was used with a second primer, which spanned a *Kpn*I site within the vector to generate a 1.6 kilobase pair fragment. This fragment was ligated to the pGEM-T vector and transformed into bacterial strain JM110 (*dam*-). The enzyme *Bcl*I is methylation sensitive. Clones containing the polymerase chain reaction-generated fragment were identified as white colonies on plates containing isopropyl 1-thio-β-D-galactopyranoside and 5-bromo-4-chloro-3-indolyl β-D-galactopyranoside. The insert was removed from the T-vector by digestion with *Bcl*I and *Kpn*I,

purified on an agarose gel, and then ligated into the vector pAlterLacY in which the 1.6 kilobase pair fragment had been removed. DNA from colonies was isolated, and the mutation was verified by double-stranded DNA sequencing. At least two independent clones were kept for further study.

The T265Y/M276Y double mutant was constructed by first creating the T265Y mutant as outlined above. The resulting pT265Y DNA was used as a template for PCR with a mutagenic primer that spans codon 276 of the *lacY* gene and a second primer, which spanned the *Kpn*I site within the vector.

DNA Sequencing. Mutations were confirmed by sequencing the appropriate regions of the *lacY* gene. Sequencing was performed on double-stranded plasmid according to Kraft et al. (*41*).

RESULTS

Mutagenesis of TMS-8. Previous work from our laboratory has shown that Pro-280, the first amino acid in the conserved loop 8−9 motif, is important for conformational changes associated with H^+/lactose transport. Several bulky substitutions at position 280 (P280M and P280L) have less than 4% transport activity (*18*). Recent studies indicate that Pro-280 is located on a side of TMS-8 shown to cross-link with TMS-5 (*21*). In the current study, we have made 30 site-directed mutants on the side of TMS-8 that cross-links with TMS-5 and contains Pro-280 (see helical wheel plot of TMS-8 in Figure 2). Our rationale was that Pro-280 may be contained within a face of TMS-8 that is important for conformational changes and that this region could be identified by substitutions that alter side-chain volume and thereby disrupt the ability of TMS-8 to properly interact with other transmembrane segments. To test this hypothesis, the following substitutions have been made: Phe-261 → (Asp/Ala/Trp); Val-264 → (Ala/Cys/Phe/Trp); Thr-265 → (Ala/Ser/Gln/Tyr); Gly-268 → (Ala/Ser/Cys/Val); Leu-271 → (Ala/Phe/Trp); Asn-272 → (Ala/Gln/Tyr); Ile-275 → (Ala/Phe/Trp); Met-276 → (Ala/Leu/Tyr); Phe-278 → (Ala/Trp); and a double mutant, Thr-265/Met-276 → Tyr-265/Tyr-276.

Expression of Mutants. Table 1 shows the expression levels of the strains containing the TMS-8 mutations. The majority of the mutants were expressed at moderate to high levels when compared to the wild-type strain. However, one codon 264 mutation (V264W) and one codon 275 mutation (I275W) had low, but detectable levels of expression.

Phenotype on MacConkey Plates. The phenotype of the mutant strains on MacConkey plates was used as a crude qualitative measurement of the effect of the mutations on transport function. Strains with mutations that render the lactose permease very defective will exhibit a white or pink phenotype on MacConkey plates. Strains with significant activity usually form red colonies. When the wild-type and mutant strains were plated on MacConkey plates containing lactose (a β-galactoside) or melibiose (an α-galactoside), some general trends were observed. Table 2 shows the plate phenotypes of the mutants arranged according to their position on the helical wheel plot shown in Figure 2 (moving clockwise starting from codon 278). Most of the mutant strains were able to transport lactose as indicated by their red phenotype on MacConkey plates containing 0.4% or 1% lactose. However, certain mutations at codon 261 (F261D), codon 272 (N272Q and N272Y), codon 265 (T265Q and T265Y), codon 276 (M276A), and the double mutant (T265Y/M276Y) were very defective, as shown by their white or pink phenotypes. The G268V mutation showed a less severe defect in lactose transport as indicated by its red center phenotype.

Table 2: Phenotype on MacConkey Plates[a]

	melibiose		lactose	
strain[b]	0.4%	1.0%	0.4%	1.0%
wild type	red	red	red	red
F278A	red center	red center	red	red
F278W	dark pink	dark pink	red	red
L271A	red	red	red	red
L271F	pink	pink	red	red
L271W	red	red	red	red
V264A	red	red	red	red
V264C	red	red	red	red
V264F	red	red	red	red
V264W	pink	pink	red	red
I275A	red	red	red	red
I275F	red	red	red	red
I275W	red	red	red	red
G268A	red	red	red	red
G268S	red	red	red	red
G268C	red	red	red	red
G268V	white	white	red center	red center
F261D	pink	pink	white	white
F261A	pink	pink	red	red
F261W	pink	pink	red	red
N272A	red	red	red	red
N272Q	pink	pink	white	white
N272Y	white	white	white	white
T265A	red	red	red	red
T265S	red	red	red	red
T265Q	dark pink	dark pink	white	white
T265Y	red center	red center	white	white
M276A	pink	pink	pink	pink
M276L	red	red	red	red
M276Y	red	red	red	red
T265Y/M276Y	pink	pink	white	white

[a] A red phenotype indicates the ability to ferment the added sugar, whereas a white phenotype indicates a lack of significant fermentation. Pink and red center reflects an intermediate level of fermentation. [b] The designated plasmids were transformed into *E. coli* strain HS4006/$F'I^QZ^+Y^-$. The transformed strains were streaked onto MacConkey plates containing the designated sugar concentration, and the color of colonies were observed the following day. The mutant strains are listed according to the helical wheel plot shown in Figure 2, beginning with Phe-278 and proceeding in the clockwise direction.

The plate phenotype results were similar for melibiose. Most of the mutant strains were able to transport melibiose as indicated by their red phenotype on MacConkey plates containing 0.4% or 1% melibiose. Again, mutations at codon 261 (F261D, F261A, and F261W), codon 272 (N272Q and N272Y), codon 265 (T265Q), codon 276 (M276A), and the double mutant (T265Y/M276Y) were very defective for melibiose transport, as shown by their white or pink phenotypes. However, unlike the results obtained with lactose, mutations at codon 278 (F278W), codon 271 (L271F), codon 264 (V264W), and codon-268 (G268V) displayed pink or white phenotypes. Furthermore, the T265Y and F278A mutants showed a less severe defect in melibiose transport as indicated by a red center phenotype.

Overall, the plate phenotype results indicate that mutations at position 272 are the most disruptive to function. The conservative substitution N272Q displayed white or pink phenotypes when grown on either sugar. Mutants with large

Table 3: Quantitative Measurement of Lactose Transport

strain[c]	downhill initial rate[a] [nmol of lactose/(min·mg of protein)]	apparent $K_m \pm$ SE[b] (mM)	apparent $V_{max} \pm$ SE [nmol of lactose/(min·mg of protein)]
pAlterLacY (wild type)	34.0 ± 3.1	0.6 ± 0.1	220.1 ± 22.0
pF278A	14.8 ± 0.8	0.2 ± 0.1	172.9 ± 18.9
pF278W	27.2 ± 1.1	0.8 ± 0.1	135.7 ± 1.1
pL271A	24.9 ± 0.9	0.3 ± 0.1	181.0 ± 3.6
pL271F	3.5 ± 0.04	0.2 ± 0.1	12.2 ± 0.7
pL271W	37.0 ± 4.0	0.2 ± 0.1	132.8 ± 7.6
pV264A	21.5 ± 2.8	0.4 ± 0.1	221.5 ± 21.0
pV264C	15.5 ± 0.8	0.7 ± 0.4	119.4 ± 30.3
pV264F	12.1 ± 1.0	2.2 ± 0.4	264.2 ± 75.4
pV264W	1.8 ± 0.2	0.5 ± 0.2	9.4 ± 3.5
pI275A	20.6 ± 0.6	0.4 ± 0.1	216.7 ± 21.4
pI275F	16.0 ± 2.0	1.4 ± 0.1	260.5 ± 77.6
pI275W	11.5 ± 1.4	1.7 ± 0.3	224.9 ± 23.4
pG268A	38.7 ± 0.9	0.6 ± 0.1	286.7 ± 33.4
pG268S	11.9 ± 0.9	<0.1	19.8 ± 2.0
pG268C	20.0 ± 0.8	2.3 ± 0.1	425.9 ± 57.5
pG268V	0.8 ± 0.1	0.8 ± 0.1	8.4 ± 0.7
pF261D	<0.1	not determined	not determined
pF261A	0.7 ± 0.1	2.4 ± 0.2	17.9 ± 0.2
pF261W	19.1 ± 0.7	<0.1	26.0 ± 2.0
pN272A	45.0 ± 1.4	0.6 ± 0.1	323.4 ± 37.3
pN272Q	1.3 ± 0.2	0.3 ± 0.1	4.5 ± 0.4
pN272Y	0.2 ± 0.1	not determined	not determined
pT265A	6.8 ± 0.2	3.6 ± 0.4	263.0 ± 7.7
pT265S	16.4 ± 0.4	2.1 ± 0.1	375.1 ± 3.8
pT265Q	0.8 ± 0.1	1.5 ± 0.3	12.0 ± 3.7
pT265Y	0.3 ± 0.1	not determined	not determined
pM276A	1.4 ± 0.1	0.2 ± 0.1	4.1 ± 0.5
pM276L	12.8 ± 0.6	1.1 ± 0.1	153.3 ± 5.4
pM276Y	11.4 ± 0.2	1.7 ± 0.3	221.1 ± 33.2
pT265Y/M276Y	<0.1	not determined	not determined

[a] Initial rates of downhill lactose transport were measured in strain HS4006/F′$I^QZ^+Y^-$ carrying the wild-type or designated mutant plasmids as described under Materials and Methods using a 0.1 mM final lactose concentration. The pH was held constant at 7.0. [b] Apparent K_m and apparent V_{max} values were determined in downhill lactose transport assays as described under Materials and Methods. [c] The mutant strains are listed according to the helical wheel plot shown in Figure 2, beginning with Phe-278 and proceeding in the clockwise direction.

alterations in side-chain volume at positions 261, 265, 268, or 276 also demonstrated severe defects in lactose or melibiose transport. As expected, the double mutant (T265Y/M276Y) displayed more severe defects than either single tyrosine mutant (T265Y or M276Y).

Downhill Lactose Transport. To obtain a quantitative measure of the transport process, *in vitro* transport experiments were conducted. Table 3 shows the results of downhill lactose transport assays that were carried out in a *lacZ*$^+$ strain, HS4006/F′Z^+Y^-, transformed with plasmid containing the wild-type or mutant *lacY* gene. The assay is termed downhill because it measures lactose transport down a sugar concentration gradient. This concentration gradient is maintained by the activity of the *lacZ* gene, which encodes β-galactosidase and cleaves the sugar so that it is rapidly metabolized once it enters the cell (*42*). As seen in Table 3, most of the mutants displaying a pink or white phenotype had low rates of transport compared to the wild-type strain. In particular, all of the mutants with a white phenotype on lactose plates (F261D, N272Q, N272Y, T265Q, T265Y, and T265Y/M276Y) were inactive for lactose transport. One mutant, N272A, had a significantly higher rate of downhill lactose transport when compared to the wild type. The low downhill lactose transport obtained with the V264W mutant may be explained by the poor expression of this mutant. However, another mutant, I275W, had a significant rate of downhill lactose transport even though its expression levels appeared lower. The occasional lack of correlation between high transport activity and low expression levels may be attributed to certain mutations making the protein unstable during the membrane isolation procedure required for Western analysis. However, in the intact cells that are used for the transport assays, the mutant protein may be quite stable (*18*).

Overall, the downhill transport results have shown that positions 261, 265, and 272 are very sensitive to changes in side-chain volume. The results for codon 276 indicate that large changes in side-chain volume are defective for transport. It is interesting to note that codons 261, 265, 272, and 276 form a continuous stripe along TMS-8. Since these mutants display moderate to high levels of expression, it is likely that these mutants exert their effects by altering the sugar recognition site and/or affecting the ability of the mutant permease to make conformational changes.

Kinetic Analysis of the Mutant and Wild-Type Strains. To determine if the mutations exert their effects by inhibiting sugar binding and/or inhibiting the velocity of lactose transport, the apparent K_m and apparent V_{max} values for lactose transport were measured in the mutant and wild-type strains. As shown in Table 3, the wild-type strain exhibited an apparent K_m for lactose of 0.6 mM with a V_{max} of 220.1 nmol of lactose/(min·mg of protein). Most of the bulky substitutions at positions 264, 271, 275, and 278 were well tolerated. The K_m for these mutants ranged from 0.2 to 2.2 mM. Furthermore, most of the mutants displayed a rate of transport that was similar to that of the wild-type strain [apparent V_{max} values ranged from 119.4 to 264.2 nmol of lactose/(min·mg of protein)]. The two exceptions were the V264W and L271F mutants, which showed apparent K_m values of 0.5 and 0.2 mM, respectively, and V_{max} values of 9.4 and 12.2 nmol of lactose/(min·mg of protein), respectively. Only these two mutants (V264W and L271F) demonstrated a severe defect in the ability to make conformational changes and/or bind sugar.

By comparison, several mutations at codons 261, 265, 268, and 272 and one codon 276 mutation exhibited significantly altered rates of lactose transport as compared to the wild-type strain. At position 261, both smaller and larger substitutions (i.e., F261A and F261W) had V_{max} values that were less than 15% of the wild-type strain. Although the apparent V_{max} value was essentially the same for these two mutants, the smaller alanine substitution displayed poor affinity for the sugar (apparent $K_m = 2.4$ mM) and the large aromatic tryptophan substitution exhibited an increased affinity for lactose (apparent $K_m < 0.1$ mM). These results suggest that mutations at codon 261 may affect both sugar recognition and conformational changes. At positions 265, 268, and 272, substitutions that were relatively conservative with regard to side-chain volume were seen to have dramatic effects. In particular, the T265Q, G268S, and N272Q strains showed apparent V_{max} values of 12.0, 19.8, and 4.5 nmol of lactose/(min·mg of protein), respectively.

Three mutants displayed an elevated rate of lactose transport when compared to the wild-type strain. The G268C,

Table 4: Uphill Transport in Wild-Type and Mutant Strains[a]

strain	uphill lactose accumulation (in/out)	strain	uphill lactose accumulation (in/out)
wild type	44.7 ± 4.5	G268V	2.1 ± 0.7
F278A	49.1 ± 1.7	F261D	0.13 ± 0.09
F278W	17.8 ± 1.4	F261A	1.4 ± 0.8
L271A	10.4 ± 0.8	F261W	1.9 ± 0.2
L271F	14.7 ± 2.4	N272A	2.0 ± 0.2
L271W	6.9 ± 0.1	N272Q	2.5 ± 0.8
V264A	13.0 ± 2.2	N272Y	0.1 ± 0.04
V264C	13.6 ± 2.4	T265A	11.4 ± 1.3
V264F	13.7 ± 0.4	T265S	14.3 ± 2.5
V264W	6.9 ± 1.3	T265Q	0.7 ± 0.2
I275A	15.9 ± 2.0	T265Y	2.4 ± 0.1
I275F	5.6 ± 1.4	M276A	1.0 ± 0.1
I275W	19.0 ± 1.4	M276L	16.7 ± 1.3
G268A	4.0 ± 1.1	M276Y	8.9 ± 0.3
G268C	4.0 ± 0.3	T265Y/M276Y	0.2 ± 0.2
G268S	12.6 ± 4.6		

[a] Lactose accumulation was measured in strain T184 carrying the wild-type or designated mutant plasmids as described under Materials and Methods at an external lactose concentration of 0.1 mM.

N272A, and T265S strains showed apparent V_{max} values of 425.9, 323.4, and 375.1 nmol/(min·mg of protein), respectively, and apparent K_m values of 2.3, 0.6, and 2.1 mM, respectively. Most of the substitutions at positions 268 and 272 had apparent K_m values close to that of wild type. The elevated K_m value obtained for T265S was typical of the reduced specificity or binding of the sugar for mutants at position 265. In general, mutations at 268, 272, and 265 displayed significant alterations in the rate of lactose transport. Only position 265 mutations consistently displayed K_m values higher than the wild-type strain regardless of the size of the amino acid substitution.

Uphill Lactose Transport. Another important aspect of H^+/lactose cotransport is the ability to accumulate sugars against a concentration gradient. To accomplish secondary active transport, the uptake of sugar must be coupled to the uptake of H^+ ions so that the proton electrochemical gradient can provide the driving force for the accumulation of sugar. Table 4 shows the uphill transport results of the wild-type and mutant strains arranged according to their position on the helical wheel plot (moving clockwise starting from codon 278). All of the mutants, except the F278A mutant, exhibited defects in active accumulation of lactose. It is apparent from the table that the uphill accumulation became lower as large side-chain volume replacements were made close to Glu-269. The mutants at codons 278, 271, 264, and 275 generally displayed higher rates of lactose accumulation than mutants at codons 261 and 272 and large side-chain volume substitutions at codons 265 and 276.

Counterflow Experiments. To further examine the importance of this face of TMS-8 with regard to conformational changes, we conducted lactose counterflow transport assays with a few mutants. The mutants V264A, L271A, and I275A were chosen because they exhibited downhill lactose transport kinetics similar to the that of the wild-type strain, and lactose accumulation at these positions (264, 271, and 275) was less than wild type but generally higher (regardless of substitution) than substitutions at other codons. Figure 3 shows the results of a counterflow assay conducted with the wild-type, V264A, L271A, and I275A strains at 23 and 16

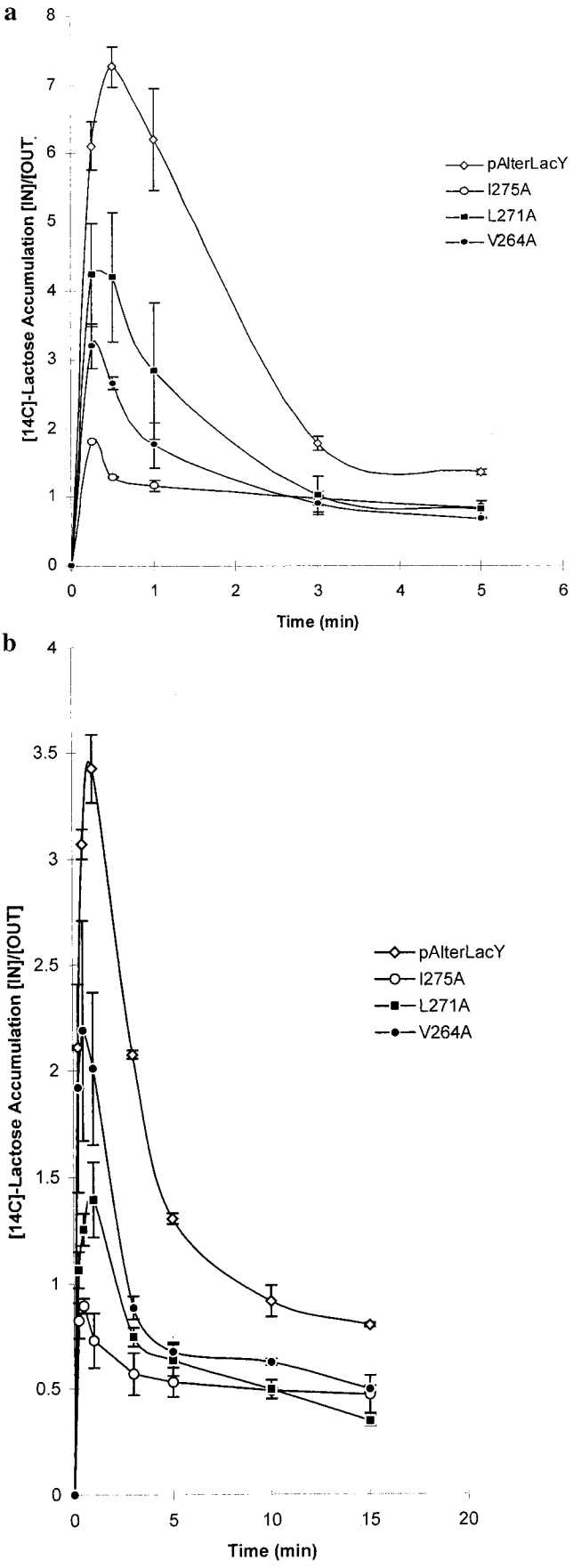

FIGURE 3: Lactose counterflow. The counterflow was measured in the wild-type (pAlterLacY), V264A, L271A, and I275A strains, as described under Materials and Methods. (a) Counterflow at 23 °C. (b) Counterflow at 16 °C.

°C. Two different temperatures were chosen to be sure that the initial rate of exchange could be accurately compared between the wild-type and mutant strains. In a counterflow assay, the cells are poisoned and preloaded with a high concentration of nonlabeled lactose. The cells are then diluted into a medium containing a low concentration of radiolabeled lactose. During the early time points, radiolabeled lactose is exchanged for nonlabeled lactose on the inside of the cell. This exchange reaction is at least 10 times more rapid than unidirectional lactose efflux and therefore leads to a plateau in which the radiolabeled lactose is accumulated against a gradient (*43*). Furthermore, at saturating external lactose concentrations, this exchange reaction appears to be insensitive to ΔpH and $\Delta\psi$ (*43*, *44*). From this observation, it has been hypothesized by others that the exchange does not require protonation and concomitant deprotonation (*43*, *44*).

As seen in Figure 3, a biphasic curve is observed for the wild-type strain. Lower temperatures slow the rate of exchange as seen with the wild-type strain which reaches equilibrium (of nonlabeled/labeled across the membrane) at about 30 s at 23 °C and 1 min at 16 °C. The results obtained for the V264A, L271A, and I275A mutants at 23 °C show that these mutants do not accumulate wild-type levels of radiolabeled lactose during the exchange portion of a counterflow assay. In particular, the I275A mutant was unable to accumulate radiolabeled lactose to a significant degree. Upon lowering the temperature to 16 °C to slow the rate of the reaction, it became even more apparent that the rate of exchange for L271A was slower than the wild-type rate of exchange. The L271A mutant also displayed a slower efflux rate (at both temperatures). At 16 °C, the L271A mutant also displayed a much lower equilibrium point of the radiolabeled/nonlabeled lactose across the membrane when compared to the results obtained at 23 °C. The counterflow assays clearly demonstrate that this face of TMS-8 is important for specific steps in the transport mechanism, and our results raise the possibility of temperature-sensitive effects on conformational changes.

DISCUSSION

There are two important conclusions obtained in the current study. First, a face on predicted TMS-8, containing Gly-268, Phe-261, Asn-272, Thr-265, and Met-276 (Figure 2, moving clockwise), plays a critical role in lactose transport activity. Mutations at these codons, which involve significant changes in side-chain volume, have detrimental effects on the initial rate of downhill transport, the maximal velocity of transport, and uphill accumulation of lactose. Several of the mutations at positions 261 and 268 and one mutant at position 265 (T265Q) showed approximately 8−26-fold decreases in apparent V_{max} when compared to the wild-type strain. The most dramatic changes in maximal velocity were observed at positions 272 and 276 in which the N272Q mutant and the M276A mutant displayed apparent V_{max} decreases of 49-fold and 54-fold, respectively, when compared to the wild-type strain. The effects on the rate of lactose transport were not all inhibitory. Some mutants along this stripe altered the rate of lactose transport such that approximately 2-fold increases in V_{max} were obtained (G268C and T265S). In general, the effects of the substitutions on the apparent K_m values for lactose transport were less dramatic, but it was noted that the K_m effects were slightly more significant for residues located close to Glu-269 on a helical wheel plot. The changes in apparent K_m values may be due to several factors such as amino acid projection into the channel, perturbation of proximal amino acids, disruption of helix packing, and altered topology of Glu-269. Previous studies have shown dramatic effects on K_m and significant changes in the rate of lactose transport when Glu-269 is altered (*30*, *45*).

According to the helical wheel plot, codons 261, 265, 268, 272, and 276 form a continuous stripe on TMS-8 (Figure 2). These residues are on the same side of TMS-8 as Pro-280, which is the first amino acid in the conserved loop 8/9 motif. Previous studies have shown that Pro-280 is important for conformational changes associated with lactose transport. Large side-chain volume substitutions (P280Y, P280M, and P280L) at this position are inhibitory to transport function (*18*). The effect of the bulky substitutions was to significantly reduce the maximal velocity of lactose transport. The results of this study combined with the previous work demonstrating the importance of the first amino acid in the loop 8/9 motif indicate that this face of TMS-8 is important for the putative conformational changes necessary for lactose transport. We previously proposed a putative conformational change involving TMS-2 sliding against TMS-11 and TMS-7 in a scissoring motion (*20*) on the basis of cross-linking data (*46*, *47*) and suppressor analysis (*17*, *20*, *48*). On the basis of the rotational symmetry of our putative model and the cross-linking studies that have been performed thus far, which show close interaction between TMS-8 and TMS-5, we now propose a similar movement of the helices at the other interface between the two halves of the protein. For example, in one conformation (i.e., the C1 conformation), TMS-8 may be relatively parallel to TMS-5, while in the other conformation (i.e., the C2 conformation), TMS-8 would lie obliquely across TMS-1 and TMS-5. During the putative conformational changes this critical face of TMS-8 may interact with residues in TMS-5 and TMS-1.

The results of the uphill transport assays further support the conclusion that this face of TMS-8 is important for conformational changes. All of the substitutions along this side of TMS-8 (except F278A) were defective for uphill transport, and uphill transport became more defective as the substitution was made closer to Glu-269 on the helical wheel plot. Thus, the side with Phe-278, Leu-271, Val-264, and Ile-275 (moving clockwise around the helical wheel plot) displayed greater accumulation of lactose than positions on the critical face of TMS-8. A clear difference emerges when the uphill transport results of this study are compared to the results obtained in our previous study of TMS-2. In the TMS-2 study (*20*), we only observed significant defects in uphill transport with mutants that displayed significant defects in downhill transport and only the critical face of TMS-2 (Ser-53, Ser-56, and Gln-60) displayed such inhibition. Thus, in the TMS-2 study there was a strong correlation between the ability to perform downhill transport and the ability to perform uphill transport. Conversely, in this study there is no strong correlation between downhill and uphill transport ability. Instead, the results indicate that the entire face is important for uphill transport with the positions on the critical face displaying slightly more inhibition of uphill transport. The most defective substitutions on the critical face were positions 261 and 272, which had less than 6% uphill

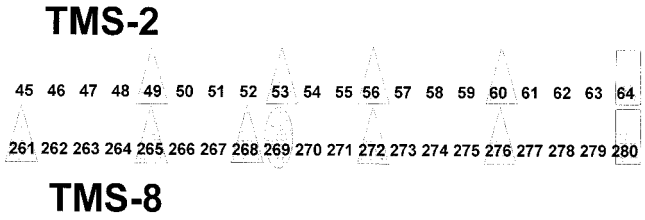

FIGURE 4: Alignment of TMS-2 from codon 45 to codon 64 with TMS-8 from codon 261 to codon 280. The first amino acid in each conserved loop motif is encased within a rectangle; the important charged residue Glu-269 is encased within a circle. Analogous positions in TMS-2 and TMS-8 that comprise a critical face important for conformational changes are encased within triangles.

transport activity. Active accumulation of lactose requires that the mutants properly couple H^+/lactose symport. We hypothesize that the presence of Glu-269 on TMS-8 may account for the difference in uphill transport between the current study and our previous one. Indeed, several other reports have shown that nonionizable substitutions at codon 269 are completely defective for active accumulation of lactose (*30*, *31*, *37*). It is possible that mutations along this face exert their effects on active accumulation of lactose by disrupting ionic interactions involving Glu-269.

The second major conclusion from this study is that the critical face of TMS-8 is located in a rotationally equivalent position to the critical face of TMS-2 identified in an earlier study (*20*). The earlier study identified a critical face on TMS-2 in the lactose permease that contained Phe-49, Ser-53, Ser-56, and Gln-60 (Figure 1). Mutations at these sites, which involved significant changes in side-chain volume, had detrimental effects on the velocity, protein expression, and/or uphill accumulation of lactose. These residues form a continuous stripe with Gly-64, which is the first amino acid in the conserved loop 2/3 motif. Figure 4 shows an alignment of TMS-2 and TMS-8 created by matching the conserved loop 2/3 and conserved loop 8/9 motif. From this alignment we can see that there is an overlap between the positions in TMS-2 and TMS-8 that comprise the critical face for conformational changes in each of these transmembrane segments. When written as codon pairs, starting with the first position in the conserved loop motif and counting backward, the alignment of important codons in each transmembrane segment looks as follows: TMS-2/TMS-8 → 64/280, 60/276, 56/272, 53/269, 52/268, 49/265, and 45/261 (also see Figure 1). We have included Glu-269 because of the background work from this laboratory, which determined that a conservative substitution of aspartate at this codon results in significant changes in apparent K_m and V_{max} values (*30*). Together with our previous mutagenesis studies of TMS-2 and TMS-8, the pairs of 64/280, 60/276, 56/272, 53/269, and 49/265 appear to be very important with regard to the velocity of lactose transport. In contrast, we found in our study involving TMS-2 that position 52 was relatively insensitive to large side-chain volume substitutions and no mutations were made at position 45 (*20*). Nevertheless, it is striking that five of the seven pairs have been shown to be important for conformational changes. It is also interesting to note that each of the codons from TMS-2 in the two pairs that do not form a match has shown some effect upon substitution. In the TMS-2 study, an I52W mutant displayed some defects in accumulation of lactose (*20*), and a cysteine replacement of codon 45 in a C-less background showed

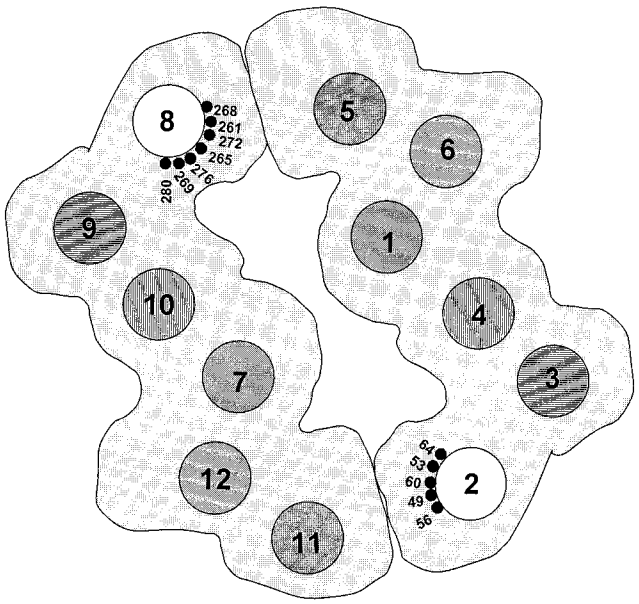

FIGURE 5: Cross-sectional model of the lactose permease. The basic features of this model were originally described in ref *14*, and a revised model that incorporated recent cross-linking and biophysical data was proposed in ref *20*. In the model shown here, the important residues in TMS-2 and TMS-8 are highlighted. As summarized in ref *20* and the introduction to this paper, these residues are thought to project toward the interface between the two halves of the permease. The hatching patterns of the helices are meant to emphasize the homology between the two halves of the permease. For example, helix 1 in the first half of the permease is equivalent to helix 7 in the second half.

greater than 60% inhibition by NEM (*49*). Overall, the codon pairs display similar trends with regard to the sensitivity of the codons to replacement. In the TMS-2 study, codons 60 and 49 were more tolerant of changes in side-chain volume in terms of initial downhill transport rates. Similarly, in this study we found that codons 276 and 265 were more tolerant of changes in terms of initial downhill transport rates. As expected, the double tyrosine mutant (T265Y/M276Y) displayed greater defects than either single tyrosine mutant at position 276 or 265 in terms of plate phenotypes and initial downhill transport rates. Therefore, experimental data support the idea that these codon pairs represent critical positions along each transmembrane segment where putative conformational changes take place (see Figure 5). The overlap of codons within the critical face of TMS-2 and TMS-8, along with the biophysical and biochemical studies placing these codons in domains of interaction with TMS-11 and TMS-5, respectively, supports the primary feature of our hypothetical structural model of the lactose permease, rotational symmetry. Furthermore, our model can be used to explain much of the experimental data obtained from this and other studies based upon the idea of positional equivalence between the two halves of the protein.

ACKNOWLEDGMENT

We thank Dr. Thomas H. Wilson for providing us with the antibody used in the experiment of Table 1 and Mrs. Elizabeth Matzke for assistance with the protein expression experiments.

REFERENCES

1. West, I. C., and Mitchell, P. (1973) *Biochem. J. 132*, 587−592.

2. West, I. C. (1970) *Biochem. Biophys. Res. Commun*. *41*, 655−661.
3. Crane, R. K. (1977) *Rev. Physiol. Biochem. Pharmacol*. *78*, 99−159.
4. Mitchell, P. (1963) *Biochem. Soc. Symp*. *22*, 142−168.
5. Teather, R. M., Muller-Hill, B., Abrutsch, U., Aichele, G., and Overath, P. (1978) *Mol. Gen. Genet*. *159*, 239−248.
6. Buchel, D. E., Gronenborg, B., and Muller-Hill, B. (1980) *Nature 283*, 541−545.
7. Foster, D. L., Boublik, M., and Kaback, H. R. (1983) *J. Biol. Chem*. *258*, 31−34.
8. Calamia, J., and Manoil, C. (1990) *Proc. Natl. Acad. Sci. U.S.A. 87*, 4937−4941.
9. King, S. C., Hansen, C. L., and Wilson, T. H. (1991) *Biochim. Biophys. Acta 1062*, 177−186.
10. Patzlaff, J. S., Moeller, J. A., Barry, B. A., and Brooker, R. J. (1998) *Biochemistry 37*, 15363−15375.
11. Griffith, J. K., Baker, M. E., Rouch, D. A., Page, M. G. P., Skurray, R. A., Paulsen, I. T., Chater, K. F., Baldwin, S. A., and Henderson, P. F. J. (1992) *Curr. Opin. Cell Biol*. *4*, 684−695.
12. Henderson, P. J. F. (1990*) J. Bioenerg. Biomembr*. *22*, 525−569.
13. Pao, S. S., Paulsen, I. T., and Saier, M. J., Jr. (1998) *Microbiol. Mol. Biol. Rev. 62*, 1−34.
14. Goswitz, V. C., and Brooker R. J. (1995) *Protein Sci. 4*, 534−537.
15. Maiden, M. C. J., Davis, E. O., Baldwin, S. A., Moore, D. C. M., and Henderson, P. J. F. (1987) *Nature 325*, 641−643.
16. Kaback, R. H., Voss, J., and Wu, J. (1997) *Curr. Opin. Struct. Biol. 7*, 537−542.
17. Jessen-Marshall, A. E., Parker, N. J., and Brooker, R. J. (1997) *J. Bacteriol*. *179*, 2616−2622.
18. Pazdernik, N. J., Jessen-Marshall, A. E., and Brooker, R. J. (1997) *J. Bacteriol*. *179*, 735−741.
19. Yamaguchi, A., Someya, Yl., and Sawai, T. (1992) *J. Biol. Chem*. *267*, 19155−19162.
20. Green, A. L., Anderson, E. J., and Brooker R. J. (2000) *J. Biol. Chem*. *275*, 23240−23246.
21. Wu, J., Hardy, D., and Kaback, H. R. (1999) *Biochemistry 38*, 2320−2325.
22. Wu, J., Perrin, D. M., Sigman, D. S., and Kaback, H. R. (1995) *Proc. Natl. Acad. Sci. U.S.A. 92*, 9186−9190.
23. Wu, J., Voss, J., Hubbell, W. L., and Kaback, H. R. (1996) *Proc. Natl. Acad. Sci. U.S.A. 93*, 10123−10127.
24. Wang, Q., Voss, J., Hubbell, W. L., and Kaback, H. R. (1998) *Biochemistry 37*, 4910−4915.
25. He, M. M., Voss, J., Hubbell, W. L., and Kaback, H. R. (1997) *Biochemistry 36*, 13682−13687.
26. Jung, K., Jung, H., Wu, J., Prive, G. G., and Kaback, H. R. (1993) *Biochemistry 32*, 12273−12278.
27. Jung, K., Voss, J., He, M., Hubbell, W. L., and Kaback, H. R. (1995) *Biochemistry 34*, 6272−6277.
28. Frillingos, S., and Kaback, H. R. (1997) *Protein Sci. 6*, 438−443.
29. Frillingos, S., Ujwal, M. L., Sun, J., and Kaback, H. R. (1997) *Protein Sci. 6*, 431−437.
30. Franco, P. J., and Brooker, R. J. (1994) *J. Biol. Chem*. *269*, 7379−7386.
31. Ujwal, M. L., Sahin-Toth, M., Persson, B., and Kaback, H. R. (1994) *Mol. Membr. Biol. 11*, 9−16.
32. Lee, J., Hwang, P. P., and Wilson, T. H. (1993) *J. Biol. Chem. 268*, 20007−20015.
33. Lee, J., Hwang, P. P., Hansen, C., and Wilson, T. H. (1992) *J. Biol. Chem*. *267*, 20758−20764.
34. Jung, K., Heinrich, J., Colacurcio, P., and Kaback, H. R. (1995) *Biochemistry 34*, 1030−1039.
35. Markgraf, M., Bocklage, H., and Muller-Hill, B. (1985) *Mol. Gen. Genet*. *198*, 473−475.
36. Seto-Young, D., Bedu, S., and Wilson, T. H. (1984) *J. Membr. Biol*. *79*, 185−193.
37. Hinkle, P. C., Hinkle, P. V., and Kaback, H. R. (1990) *Biochemistry 29*, 10989−10994.
38. Miller, J. (1972) *Experiments in Molecular Genetics*, p 433, Cold Spring Harbor Laboratory, Cold Spring Harbor, NY.
39. Segel, I. (1975) *Enzyme Kinetics*, Wiley and Interscience, New York.
40. Sambrook, J., Fritsch, E. F., and Maniatas, T. (1989) *Molecular Cloning: A Laboratory Manual*, Cold Spring Harbor Laboratory, Cold Spring Harbor, NY.
41. Kraft, R., Tardiff, J., Drauter, K. S., and Leinwand, L. A. (1988) *BioTechniques 6*, 544−547.
42. Rickenberg, H. V., Cohen, G., Buttin, G., and Monod, J. (1956) *Ann. Inst. Pasteur (Paris) 91*, 829−857.
43. Kaczorowski, G. J., and Kaback, H. R. (1979) *Biochemistry 18*, 3691−3697.
44. Kaczorowski, G. J., Robertson, D. E., and Kaback, H. R. (1979) *Biochemistry 18*, 3697−3704.
45. Johnson, J. L., and Brooker, R. J. (1999) *J. Biol. Chem*. *274*, 4074−4081.
46. Wu, H., Hardy, D., and Kaback, H. R. (1998) *J. Mol. Biol*. *282*, 959−967.
47. Wu, H., and Kaback, H. R. (1997) *J. Mol. Biol*. *270*, 285−293.
48. Jessen-Marshall, A. E., and Brooker, R. J. (1996) *J. Biol. Chem*. *271*, 1400−1404.
49. Frillingos, S., Sahin-Toth, M., Wu, J., and Kaback, H. R. (1998) *FASEB J. 12*, 1281−1299.
50. Teather, R. M., Bramhall, J., Riede, I., Wright, J. K., Furst, M., Aichele, G., Wilhelm, U., and Overath, P. (1980) *Eur. J. Biochem. 108*, 223−231.
51. Brooker, R. J., and Wilson, T. H. (1985) *Proc. Natl. Acad. Sci. U.S.A. 82*, 3959−3963
52. Jones, D. T., Taylor, W. R., and Thornton, J. M. (1994) *Biochemistry 33*, 3038−3049.

BI0109055